Sensitivity, quantum limits, and quantum enhancement of noise spectroscopies

Vito Giovanni Lucivero,[1] Aleksandra Dimic,[1,2] Jia Kong,[1] Ricardo Jiménez-Martínez,[1] and Morgan W. Mitchell[1,3]

[1] *ICFO-Institut de Ciencies Fotoniques, The Barcelona Institute of Science and Technology, 08860 Castelldefels (Barcelona), Spain**

[2] *Faculty of Physics, University of Belgrade, Studentski Trg 12-16, 11000 Belgrade, Serbia*

[3] *ICREA – Institució Catalana de Recerca i Estudis Avançats, 08015 Barcelona, Spain*

(Dated: October 10, 2016)

We study the fundamental limits of noise spectroscopy using estimation theory, Faraday rotation probing of an atomic spin system, and squeezed light. We find a simple and general expression for the Fisher information, which quantifies the sensitivity to spectral parameters such as resonance frequency and linewidth. For optically-detected spin noise spectroscopy, we find that shot noise imposes "local" standard quantum limits for any given probe power and atom number, and also "global" standard quantum limits when probe power and atom number are taken as free parameters. We confirm these estimation theory results using non-destructive Faraday rotation probing of hot Rb vapor, observing the predicted optima and finding good quantitative agreement with a first-principles calculation of the spin noise spectra. Finally, we show sensitivity beyond the atom- and photon-number-optimized global standard quantum limit using squeezed light.

arXiv:1610.02356v1 [quant-ph] 7 Oct 2016

Noise spectroscopies, in which naturally occurring fluctuations of a system of interest are recorded by a non-invasive probe, have applications in a wide range of disciplines including atomic [1] and solid state physics [2, 3], surface science [4], cell biology [5, 6], molecular biophysics [7, 8], geophysics [9], space science [10], quantum optomecanics [11], and quantum information processing [12–16]. By the fluctuation-dissipation theorem, the noise spectrum under thermal equilibrium gives the same information as do driven spectroscopies, with the advantage of characterizing the system in its natural, undisturbed state [17].

An important special case is spin noise spectroscopy (SNS), a versatile technique that measures magnetic resonance features from thermal spin fluctations [18]. Non-optical SNS based on resonance force microscopy [19, 20] and NV-center magnetometry [21–23] have recently emerged, but still the most widely used technique is optical Faraday rotation (FR) to detect spin orientation [24]. This FR-SNS is used to study spin physics in atomic gases [1, 25] as well as conduction electrons [26] and localized states in semiconductors [27, 28]. Extensions of SNS include measurements of cross-correlations of heterogeneous spin systems [29, 30], spin dynamics beyond thermal equilibrium [31] and multidimensional SNS [32, 33], see [34] for a review.

Understanding the statistical sensitivity of noise spectroscopies is a prerequisite for their use to constrain physical models. Because the signal is weaker than in driven spectroscopies, quantum statistical fluctuations such as shot noise often determine the sensitivity [28, 35]. A general framework to estimate the spectra of noisy classical forces influencing quantum systems has been applied to spectroscopy by homodyne detection of an externally-imposed noisy phase [36]. This framework provides fundamental limits but can be applied to noise spectroscopies only in the weak probing regime, due to the assumed "classical," i.e., imperturbable, nature of the estimated force.

Here we derive the sensitivity of noise spectroscopy with no classicality assumption about the noise source, to obtain a very simple expression for the variance of spectral parameters estimated from noise, e.g., the uncertainty on a magnetic resonance linewidth obtained by fitting a spin noise spectrum. In the case of spin noise spectroscopy, we show two results concerning the quantum limits of the technique: first, in contrast to most problems in quantum limited sensing, availability of unlimited particle-number resources does not lead to unlimited sensitivity, and second, the number-optimized classical sensitivity can be surpassed using squeezed-light probes. These theoretical predictions are tested by comparison against FR-SNS of hot rubidium vapor using a quantum-noise-limited probing system [35] and atom-resonant optical squeezing [37, 38].

Sensitivity to spectral parameters — Noise spectroscopies record an observable $Y(t)$ that carries information about the physical system of interest. Statistically, $Y(t)$ is a stationary random process with the long-time power spectral density $f(\nu, \mathbf{v})$, where f describes a family of possible spectra, ν is the linear frequency and $\mathbf{v}$ is a vector of unknown parameters. $Y(t)$ is sampled at times $t_m = m\Delta$, $m \in \mathbb{N}$ for a time T, to obtain the discrete power spectrum $S_i \equiv S(\nu_i) = |\tilde{Y}(\nu_i)|^2$, where $\tilde{Y}(\nu_i)$ is the discrete Fourier transform of $Y(t_m)$. Here $\nu_i = i\nu_T$ are discrete frequencies with separation $\nu_T \equiv 1/T$. When the acquisition is long relative to the coherence time of the noise process, so that the features of the spectrum are broad relative to ν_T, we can take $\mathrm{cov}(S_i, S_j) = 0$ for $i \neq j$ [39, 40], while $\mathrm{var}(S_i) = \langle S_i \rangle^2$. This describes a unit signal-to-noise ratio (SNR) for S_i, independent of its true value, in marked contrast to most physical estimation problems.

Two averaging procedures are often applied to re-

duce the uncertainty of S_i, and thus increase SNR: a simple averaging of $N_{\rm ave}$ independently acquired spectra $S^{(k)}$, and a "coarse-grained" averaging of $N_{\rm bin} \equiv \nu_{\rm bin}/\nu_T$ adjacent values, giving the coarse-grained spectrum $\bar{S}_i \equiv (N_{\rm bin}N_{\rm ave})^{-1}\sum_{j=1}^{N_{\rm bin}}\sum_{k=1}^{N_{\rm ave}} S^{(k)}_{iN_{\rm bin}+j}$. This averaging of $\mathcal{N} \equiv N_{\rm bin}N_{\rm ave}$ uncorrelated contributions gives $\mathrm{var}(\bar{S}_i) = \langle\bar{S}_i\rangle^2/\mathcal{N}$. By the central limit theorem, with increasing $\mathcal{N}$ the distribution of $\bar{S}_i$ rapidly approaches a multivariate normal distribution with mean $\mu_i \equiv \langle\bar{S}_i\rangle = f(\nu_i, \mathbf{v}) \equiv f_i$ and covariance matrix

$$\Sigma_{ij} \equiv \langle(\bar{S}_i - \mu_i)(\bar{S}_j - \mu_j)\rangle = \mathcal{N}^{-1} f_i^2 \delta_{ij}. \qquad (1)$$

Due to this normality, $\hat{\mathbf{v}}$ the maximum-likelihood estimator (MLE) of $\mathbf{v}$ is found by a fit that minimizes $\chi^2 \equiv \sum_i (1 - \bar{S}_i/f_i)^2$ by choice of $\mathbf{v}$. For large $\mathcal{N}$, this estimate saturates the Cramer-Rao bound [41], so that the error covariance matrix $\Gamma_{ab} \equiv \langle(\hat{\mathbf{v}}_a - \mathbf{v}_a)(\hat{\mathbf{v}}_b - \mathbf{v}_b)\rangle$ is simply $\Gamma = \mathcal{I}^{-1}$, where $\mathcal{I}$ is the Fisher information matrix for a vector-parametrized multivariate normal distribution [42]:

$$\begin{aligned}\mathcal{I}_{jk} &= \sum_i (\partial_j\mu_i)\Sigma^{-1}(\partial_k\mu_i) + \frac{1}{2}\mathrm{Tr}\left[\Sigma^{-1}(\partial_j\Sigma)\Sigma^{-1}(\partial_k\Sigma)\right] \\ &= \mathcal{N}\sum_i (\partial_j f_i) f_i^{-2} (\partial_k f_i) + \frac{1}{2}\sum_i f_i^{-4}(\partial_j f_i^2)(\partial_k f_i^2) \\ &= (\mathcal{N}+2)\sum_i f_i^{-2}(\partial_j f_i)(\partial_k f_i), \qquad (2)\end{aligned}$$

the second line following from Eq. (1).

We note that the width of the bins, which affects both $\mathcal{N}$ and the number of terms in $\sum_i$, does not alter $\mathcal{I}$, provided the graining is not so coarse as to blur the spectral features. This justifies treating the sums as integrals. We arrive to our first main result, the statistical sensitivity of spectral parameter estimation by noise spectroscopy:

$$\begin{aligned}\mathcal{I}_{jk} &= (\mathcal{N}+2)\sum_i (\partial_j \ln f_i)(\partial_k \ln f_i) \\ &\approx \frac{(\mathcal{N}+2)}{\nu_T}\int_{\nu_1}^{\nu_2} d\nu\, (\partial_j \ln f_i)(\partial_k \ln f_i) \qquad (3)\end{aligned}$$

where ν_1, ν_2 delimit the frequency range over which the fit is performed [43].

Validation — To test the applicability of this result, we analyze atomic vapor spin noise detected by FR-SNS in hot atomic vapor (see Fig. 1), using the experimental system described in [35]. As described there, the spectrum $f(\nu, \mathbf{v})$ is

$$f(\nu, \mathbf{v}) = S_{\rm ph} + S_{\rm at}\frac{(\Delta\nu)^2}{4(\nu - \nu_L)^2 + (\Delta\nu)^2} \qquad (4)$$

where $S_{\rm ph}$ is the shot-noise background, $S_{\rm at}$ is the peak atomic noise contribution, ν_L is the ^{85}Rb Larmor frequency, and $\Delta\nu$ is the magnetic resonance linewidth. As described in the Supplementary Information (SI) and in [35], $\mathbf{v}$ can be computed from the atomic number density n and probe power P, allowing first-principles computation of the covariance matrix $\Gamma^{\rm th}$ through Eq. (3).

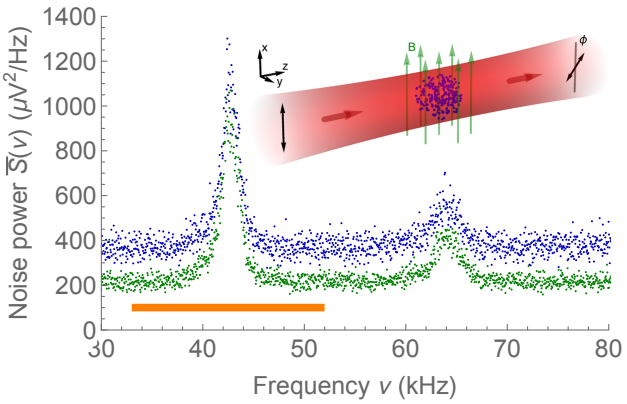

FIG. 1. Representative noise spectra showing spin noise resonances of ^{85}Rb at 42.6 kHz and ^{87}Rb at 64.0 kHz. Upper spectrum (blue) with coherent-state probing, lower spectrum (green) with polarization-squeezed probe light. Each spectrum is an average of $N_{\rm ave} = 5$ acquisitions with coarse-graining of $N_{\rm bin} = 20$. Data acquired with $n = 4.23\times10^{12}$ cm^{-3} and $P = 2.0$ mW. It is clearly seen that the noisiness $\mathrm{var}[\bar{S}(\nu)]$ of the spectrum increases with increasing $\langle\bar{S}(\nu)\rangle$. The squeezed probe reduces the shot-noise background, with a beneficial effect on both the signal-to-noise ratio and the precision of spectral parameter estimation. Orange bar below spectra shows fit region. Inset: principle of spin noise measurement. Polarized light experiences Faraday rotation by an angle ϕ proportional to the on-axis magnetization of the atomic ensemble, and is detected with a polarimeter (not shown).

A representative experimental spectrum, with $n = 4.23\times10^{12}$ cm^{-3}, $P = 2.0$ mW, $T = 500$ ms and $\Delta = 5$ µs, is shown in Fig. 1, after averaging $N_{\rm ave} = 5$ and coarse-graining $N_{\rm bin} = 20$. In these same conditions we acquired $N = 100$ such spin noise spectra with $N_{\rm ave} = 1$ and $N_{\rm bin} = 50$, and performed maximum-likelihood fits of $f(\nu, \mathbf{v})$ from Eq. (4) over the range 33 − 52 kHz, which covers the ^{85}Rb resonance at $\nu_L = 42.6$ kHz. This gives $N = 100$ samples $\mathbf{v}^{(i)}$ of the vector $\mathbf{v}$, from which we calculate the sample mean $\bar{\mathbf{v}} \equiv \sum_{i=1}^N \mathbf{v}^{(i)}/N$ and $\Gamma^{\rm exp}_{ab} \equiv \sum_{i=1}^N (v_a^{(i)} - \bar{v}_a^{(i)})(v_b^{(i)} - \bar{v}_b^{(i)})/N$, the maximum likelihood estimate (MLE) of the covariance matrix, to find

$$\Gamma^{\rm exp} = \begin{pmatrix} 32.7 & 29 & 0.06 & -349 \\ 29 & 2290 & 490 & -142000 \\ 0.06 & 490 & 3590 & -6680 \\ -349 & -142000 & -6680 & 21500 \end{pmatrix} \qquad (5)$$

where the ordering is $\mathbf{v} = (S_{\rm ph}, \nu_L, S_{\rm at}, \Delta\nu)$ with units μV^2/Hz for $S_{\rm ph}$ and $S_{\rm at}$ and Hz for ν_L and $\Delta\nu$, so that, e.g., the $(1,2)$ entry has units μV^2. The covariance

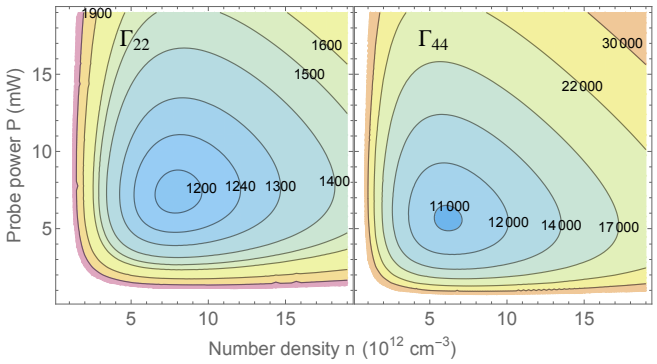

FIG. 2. $\Gamma^{\rm th}_{22}$ (left), variance in estimated line center and $\Gamma^{\rm th}_{44}$ (right), variance in estimated linewidth as predicted by Eq. (3) as a function of number density and probe power. Both in units of Hz^2. The respective optima are $\Gamma^{\rm th}_{22} = 1190$ Hz^2 and $\Gamma^{\rm th}_{44} = 10914$ Hz^2.

matrix predicted by Eq. (3) is

$$\Gamma^{\rm th} = \begin{pmatrix} 32.4 & 0.13 & 0.44 & -387 \\ 0.13 & 1990 & 0.11 & -130 \\ 0.44 & 0.11 & 3510 & -5790 \\ -387 & -130 & -5790 & 17000 \end{pmatrix}. \quad (6)$$

To compare these, we note that N p-dimensional vectors drawn from a multivariate normal distribution with covariance matrix $\Gamma^{\rm th}$ give rise to a MLE covariance matrix $\Gamma^{\rm MLE}$ with $N\Gamma^{\rm MLE}$ described by the Wishart distribution $W_p(\Gamma^{\rm th}, N)$, so that elements of $\Gamma^{\rm MLE}$ have variances $(\sigma^{\rm th}_{ij})^2 \equiv {\rm var}(\Gamma^{\rm MLE}_{ij}) = [(\Gamma^{\rm th}_{ij})^2 + \Gamma^{\rm th}_{ii}\Gamma^{\rm th}_{jj}]/N$ [44]. Explicitly, the standard deviations are

$$\sigma^{\rm th} = \begin{pmatrix} 4.6 & 25 & 0.34 & 84 \\ 25 & 280 & 260 & 58000 \\ 0.34 & 260 & 500 & 960 \\ 84 & 58000 & 960 & 2400 \end{pmatrix} \quad (7)$$

with the same units as $\Gamma^{\rm th}$, $\Gamma^{\rm exp}$. The normalized absolute deviation $|\Gamma^{\rm th}_{ij} - \Gamma^{\rm exp}_{ij}|/\sigma^{\rm th}_{ij}$ is ~ 1 for all elements, with the largest such deviation being 2.4, indicating good agreement of theory with experiment. Acquiring and analyzing spectra over the (n, P) ranges 1.49×10^{12} cm$^{-3} \leq n \leq 12.6 \times 10^{12}$ cm^{-3} and 0.5 mW $\leq P \leq 4$ mW, we find that similar agreement is seen over the whole range.

Applications in spin noise spectroscopy — We now apply our result for the sensitivity of noise spectroscopy, Eq. (3), to study the standard quantum limits of FR-SNS. For any given (n, P), the sensitivity given by Eq. (3) and Eq. (4) describes a standard quantum limit, in the sense that the readout noise $S_{\rm ph}$ is at the shot-noise level, and cannot be reduced by classical techniques. We will refer to this as a "local" standard quantum limit, because it applies to a specific point in (n, P) space.

As described in our previous work [35] the parameters $\mathbf{v}$ that appear in Eq. (4) have the following dependencies

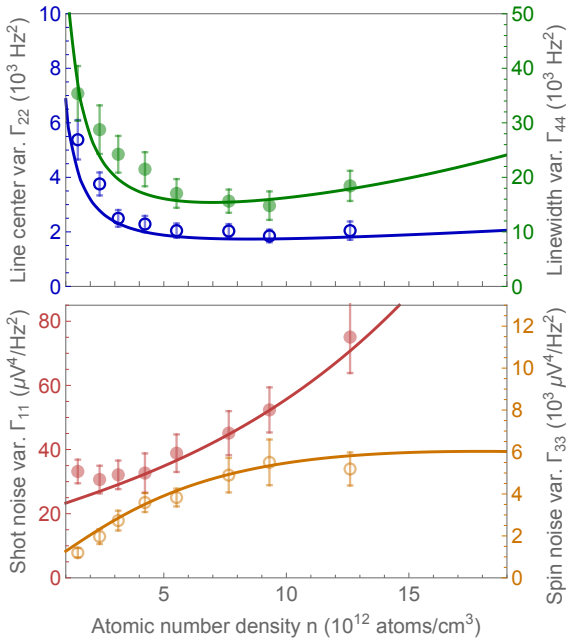
Line center var. Γ_{22} (10^3 Hz^2)
Linewidth var. Γ_{44} (10^3 Hz^2)
Shot noise var. Γ_{11} (μV^4/Hz^2)
Spin noise var. Γ_{33} (10^3 μV^4/Hz^2)
Atomic number density n (10^{12} atoms/cm^3)

FIG. 3. Sensitivity of spin noise spectroscopy versus atomic density in theory and experiment. Optical power is $P = 2$ mW throughout. (a) Lower, blue curve shows Γ_{22}, the variance of the Larmor frequency estimate, computed by Eq. (3) and from experiment (blue hollow circles), on left (blue) axis. Upper, green curve shows Γ_{44}, the variance of the linewidth estimate, and observed variance (green filled circles), on right (green) axis. (b) Upper, red curve shows Γ_{11}, the variance of the shot noise estimate, from theory and from experiment (red filled circles), on left (red) axis. Lower, orange curve shows Γ_{33}, the variance of the spin noise estimate, and observed variance (orange hollow circles), on right (orange) axis. Error bars show plus/minus one standard error (see SI).

on (n, P): $S_{\rm at} \propto P^2 n/\Delta\nu$, $\Delta\nu = \Delta\nu_0 + An + BP$, where A and B are constants describing collisional and power broadening, respectively, and $S_{\rm ph} \propto P\xi^2$, where ξ^2 is the squeezing parameter, with $\xi^2 = 1$ indicating the shot noise level. ν_L is to good approximation independent of (n, P) in the ranges we study. This form, a white noise background plus a Lorentzian spectral feature subject to line broadening with increasing probe power is found in solid state [28] as well as atomic systems. Both broadening and narrowing of resonance lines with increasing dopant concentration is observed in solid state systems [45].

These (n, P) dependencies, along with the fundamental sensitivity given in Eq. (3), create global optima for the sensitivity to ν_L and $\Delta\nu$. This is in stark contrast to textbook quantum-limited estimation problems, in which increasing particle number allows arbitrarily small uncertainties. The optimum can be understood via the dependence of SNR and line broadening on P and n: at low values, SNR increases as the product of these, while line broadening is negligible. At high P or n, the SNR sat-

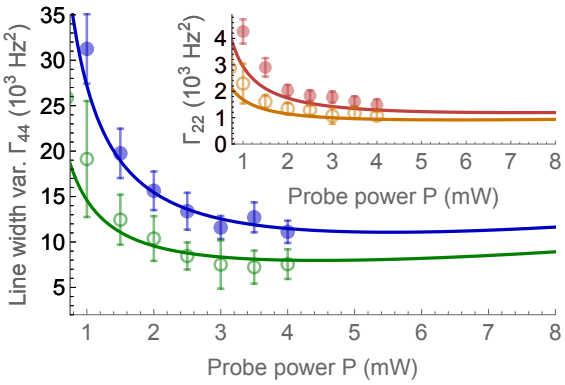

FIG. 4. Sensitivity of spin noise spectroscopy versus probe power, and sensitivity enhancement by squeezing. Atom number density is $n = 7.65 \times 10^{12}$ cm^{-3} throughout. Main plot: variance $\Gamma_{44}^{\rm exp}$ of the linewidth estimate, versus power for a coherent-state probe by Eq. (3) (upper, blue curve) and experiment (blue filled circles). Same quantities with a polarization squeezed probe with 2.6 dB of squeezing by Eq. (3) (green, lower curve) and experiment (green hollow circles). Error bars show plus/minus one standard error. Inset shows the same quantities for $\Gamma_{22}^{\rm exp}$, the variance of the Larmor frequency estimate.

urates while the line broadening increases without limit, reducing sensitivity. An intermediate condition gives the optimum. Similar line broadening considerations determine the optima for optical magnetometers [46–48].

As shown in Fig. 2, for our ^{85}Rb system, the optima are near $(n, P) = (7 \times 10^{12}\ \text{cm}^{-3}, 7\ \text{mW})$. Experimental exploration of these optima is shown in Figs. 3 and 4. These represent the standard quantum limit, not for a particular (n, P), but rather over the whole (n, P) parameter space. For this reason, we refer to these as the "global" standard quantum limits for our system.

Sensitivity enhancement by squeezing — The existence of global optima motivates the use of optical squeezing, which promises a way to improve statistical sensitivity when the improvement by choice of particle number is exhausted. It is not a foregone conclusion that squeezing will help, however: in other applications of squeezed light to probe high-density ensembles [49], squeezing had no beneficial effect at the optimum. Using a sub-threshold OPO described in [35, 37], we generate 2.6 dB of polarization squeezing, or $\xi^2 = 0.55$, and observe a reduction of $\Gamma_{22}^{\rm exp}$ and $\Gamma_{44}^{\rm exp}$ by a factor 0.61, constant to within uncertainties, as shown in Fig. 4. The four $\Gamma_{44}^{\rm exp}$ measurements from 2.5 mW to 4 mW are in total 7.0 standard deviations below 10914 Hz^2, the global standard quantum limit for our system. The optimum with squeezing also occurs at lower probe power than the optimum without squeezing. This leads to less line broadening and more generally to a less invasive measurement.

Conclusions — We have derived the sensitivity of noise spectroscopies from estimation theory, finding simple expressions for the Fisher information matrix in terms of the spectral model. The result enables rigorous use of noise spectra in cell biology [5, 6], molecular biophysics [7, 8], geophysics [9], space science [10], and quantum information processing [12–16]. For optically-probed particulate systems that show line-broadening, e.g. atomic vapors and quasiparticle systems in solid state physics, the theory predicts global sensitivity optima as a function of particle number density and probe power. These global standard quantum limits define the limiting sensitivity of noise spectroscopy given unlimited classical resources. We quantitatively validate the theory and confirm the prediction of global optima for spin noise spectroscopy of a hot atomic vapor probed by optical Faraday rotation. Using a polarization-squeezed probe beam, we surpass the global standard quantum limit for this system.

This work was supported by European Research Council (ERC) projects AQUMET (280169) and ERIDIAN (713682); European Union QUIC (641122); Ministerio de Economa y Competitividad (MINECO) Severo Ochoa programme (SEV-2015-0522) and projects MAQRO (Ref. FIS2015-68039-P), XPLICA (FIS2014-62181-EXP); Agència de Gestió d'Ajuts Universitaris i de Recerca (AGAUR) project (2014-SGR-1295); Fundació Privada CELLEX; RJM was supported by the Marie Sklodowska-Curie fellowship project QUTEMAG (654339).

* Corresponding author: lucivero@princeton.edu ; Current address: Department of Physics, Princeton University, Princeton, New Jersey 08544, USA

[1] S. A. Crooker, D. G. Rickel, A. V. Balatsky, and D. L. Smith, Nature **431**, 49 (2004).
[2] J. Sikula and L. Stourac, in *MIEL 2002. 23rd International Conference on Microelectronics*, Vol. 2 (2002) pp. 767–772 vol.2.
[3] S. A. Vitusevich, M. V. Petrychuk, A. M. Kurakin, S. V. Danylyuk, D. Mayer, Z. Bougrioua, A. V. Naumov, A. E. Belyaev, and N. Klein, Journal of Statistical Mechanics: Theory and Experiment **2009**, P01046 (2009).
[4] Y. Romach, C. Müller, T. Unden, L. J. Rogers, T. Isoda, K. M. Itoh, M. Markham, A. Stacey, J. Meijer, S. Pezzagna, B. Naydenov, L. P. McGuinness, N. Bar-Gill, and F. Jelezko, Phys. Rev. Lett. **114**, 017601 (2015).
[5] I. M. Tolić-Nørrelykke, E.-L. Munteanu, G. Thon, L. Oddershede, and K. Berg-Sørensen, Phys. Rev. Lett. **93**, 078102 (2004).
[6] M. A. Taylor, J. Knittel, and W. P. Bowen, New Journal of Physics **15**, 023018 (2013).
[7] M. Kawakami, K. Byrne, B. Khatri, T. C. B. Mcleish, S. E. Radford, and D. A. Smith, Langmuir **20**, 9299 (2004).
[8] K. Berg-Sørensen and H. Flyvbjerg, Review of Scientific Instruments **75**, 594 (2004).
[9] A. V. Descherevsky, A. A. Lukk, A. Y. Sidorin, G. V. Vstovsky, and S. F. Timashev, Natural Hazards and Earth System Science **3**, 159 (2003).

[10] M. Moncuquet, A. Lecacheux, N. Meyer-Vernet, B. Cecconi, and W. S. Kurth, Geophysical Research Letters **32** (2005), 10.1029/2005GL022508, l20S02.

[11] A. H. Safavi-Naeini, J. Chan, J. T. Hill, T. P. M. Alegre, A. Krause, and O. Painter, Phys. Rev. Lett. **108**, 033602 (2012).

[12] M. J. Biercuk, H. Uys, A. P. VanDevender, N. Shiga, W. M. Itano, and J. J. Bollinger, Nature **458**, 996 (2009).

[13] G. A. Álvarez and D. Suter, Phys. Rev. Lett. **107**, 230501 (2011).

[14] T. Yuge, S. Sasaki, and Y. Hirayama, Phys. Rev. Lett. **107**, 170504 (2011).

[15] J. Bylander, S. Gustavsson, F. Yan, F. Yoshihara, K. Harrabi, G. Fitch, D. G. Cory, Y. Nakamura, J.-S. Tsai, and W. D. Oliver, Nat Phys **7**, 565 (2011).

[16] J. Medford, L. Cywiński, C. Barthel, C. M. Marcus, M. P. Hanson, and A. C. Gossard, Phys. Rev. Lett. **108**, 086802 (2012).

[17] G. E. Katsoprinakis, A. T. Dellis, and I. K. Kominis, Phys. Rev. A **75**, 042502 (2007).

[18] V. S. Zapasskii, A. Greilich, S. A. Crooker, Y. Li, G. G. Kozlov, D. R. Yakovlev, D. Reuter, A. D. Wieck, and M. Bayer, Phys. Rev. Lett. **110**, 176601 (2013).

[19] D. Rugar, R. Budakian, H. J. Mamin, and B. W. Chui, Nature **430**, 329 (2004).

[20] R. Budakian, H. J. Mamin, B. W. Chui, and D. Rugar, Science **307**, 408 (2005).

[21] G. Balasubramanian, I. Y. Chan, R. Kolesov, M. Al-Hmoud, J. Tisler, C. Shin, C. Kim, A. Wojcik, P. R. Hemmer, A. Krueger, T. Hanke, A. Leitenstorfer, R. Bratschitsch, F. Jelezko, and J. Wrachtrup, Nature **455**, 648 (2008).

[22] J. R. Maze, P. L. Stanwix, J. S. Hodges, S. Hong, J. M. Taylor, P. Cappellaro, L. Jiang, M. V. G. Dutt, E. Togan, A. S. Zibrov, A. Yacoby, R. L. Walsworth, and M. D. Lukin, Nature **455**, 644 (2008).

[23] H. J. Mamin, M. H. Sherwood, and D. Rugar, Phys. Rev. B **86**, 195422 (2012).

[24] B. Aleksandrov and V. S. Zapasskii, Sov. Phys. JETP **54**, 64 (1981).

[25] G. E. Katsoprinakis, A. T. Dellis, and I. K. Kominis, Phys. Rev. A **75**, 042502 (2007).

[26] M. Oestreich, M. Römer, R. J. Haug, and D. Hägele, Phys. Rev. Lett. **95**, 216603 (2005).

[27] S. A. Crooker, J. Brandt, C. Sandfort, A. Greilich, D. R. Yakovlev, D. Reuter, A. D. Wieck, and M. Bayer, Phys. Rev. Lett. **104**, 036601 (2010).

[28] P. Glasenapp, A. Greilich, I. I. Ryzhov, V. S. Zapasskii, D. R. Yakovlev, G. G. Kozlov, and M. Bayer, Phys. Rev. B **88**, 165314 (2013).

[29] A. T. Dellis, M. Loulakis, and I. K. Kominis, Phys. Rev. A **90**, 032705 (2014).

[30] D. Roy, L. Yang, S. A. Crooker, and N. A. Sinitsyn, Scientific Reports **5**, 9573 (2015).

[31] P. Glasenapp, N. Sinitsyn, L. Yang, D. Rickel, D. Roy, A. Greilich, M. Bayer, and S. Crooker, Phys. Rev. Lett. **113**, 156601 (2014).

[32] S. T. Cundiff and S. Mukamel, Physics Today **66**, 44 (2013).

[33] M. Kryvohuz and S. Mukamel, The Journal of Chemical Physics **142**, 212430 (2015), 10.1063/1.4917527.

[34] N. A. Sinitsyn and Y. V. Pershin, Reports on Progress in Physics **79**, 106501 (2016).

[35] V. G. Lucivero, R. Jiménez-Martínez, J. Kong, and M. W. Mitchell, Phys. Rev. A **93**, 053802 (2016).

[36] S. Ng, S. Z. Ang, T. A. Wheatley, H. Yonezawa, A. Furusawa, E. H. Huntington, and M. Tsang, Phys. Rev. A **93**, 042121 (2016).

[37] A. Predojevic, Z. Zhai, J. M. Caballero, and M. W. Mitchell, Phys. Rev. A **78**, 063820 (2008).

[38] F. Wolfgramm, A. Cerè, F. A. Beduini, A. Predojević, M. Koschorreck, and M. W. Mitchell, Phys. Rev. Lett. **105**, 053601 (2010).

[39] W. L. Root and T. S. Pitcher, Ann. Math. Statist. **26**, 313 (1955).

[40] M. Hamidi and J. Pearl, IEEE Transactions on Information Theory **21**, 480 (1975).

[41] M. Levin, IEEE Transactions on Information Theory **11**, 100 (1965).

[42] A. Klein, G. Mélard, and T. Zahaf, Linear Algebra and its Applications **321**, 209 (2000), eighth Special Issue on Linear Algebra and Statistics.

[43] A similar result is given in Eq. (2.32) of [36]. Two important points of difference: The expression in [36] describes the *quantum Fisher information*, i.e., the information available under the best possible measurement, while ours indicates the Fisher information *per se*, the information of the measurement actually made. Also, our result involves the parameter dependence of f, including noise due to the probe, whereas that of [36] includes only S_X, the noise of the external force.

[44] J. Wishart, Biometrika **20A (1-2)**, 32 (1928).

[45] J. Hübner, F. Berski, R. Dahbashi, and M. Oestreich, physica status solidi (b) **251**, 1824 (2014).

[46] D. Budker, V. Yashchuk, and M. Zolotorev, Phys. Rev. Lett. **81**, 5788 (1998).

[47] D. Budker and M. Romalis, Nat Phys **3**, 227 (2007).

[48] S. Pustelny, A. Wojciechowski, M. Gring, M. Kotyrba, J. Zachorowski, and W. Gawlik, Journal of Applied Physics **103**, 063108 (2008).

[49] T. Horrom, R. Singh, J. P. Dowling, and E. E. Mikhailov, Phys. Rev. A **86**, 023803 (2012).

[50] J. Kenney and E. Keeping, *Mathematics of statistics part II*, 2nd ed. (Chapman and Hall, London, 1939).

Supplementary Material for *Sensitivity, quantum limits, and quantum enhancement of noise spectroscopies* by Lucivero *et al.*

STATISTICS OF S.

We first note that if $Y(t)$ is a stationary gaussian random process, so that $P(Y(t_1+\tau)=y_1, Y(t_2+\tau)=y_2, \ldots, Y(t_n+\tau)=y_n)$ is normally distributed and independent of τ, then its Fourier transform $\tilde{Y}(\nu_j) \equiv \sum_m \exp[i\nu_j t_m] Y(t_m)$ (for brevity we omit normalization) has the following properties. Writing $\tilde{Y}(\nu_j) = x_j + iy_j = r_j \exp[i\theta_j]$ with real x, y, r and $\theta \in [0, 2\pi)$, linearity of the sum implies that x_j and y_j are normally distributed. For $\nu_j \neq 0$, stationarity implies $\tilde{Y}(\nu_j) = \sum_m \exp[i\nu_j(t_m+\tau)] Y(t_m) = \exp[i\nu_j\tau]\tilde{Y}(\nu_j)$, independently of the value of τ. As a consequence, θ_j must be uniformly distributed on $[0, 2\pi)$. This phase invariance implies equal distributions for x and y, and that $r_j^2/\sigma_x^2 = (x_j^2+y_j^2)/\sigma_x^2$ is described by the chi-squared distribution χ_k^2 with $k=2$, since x_j/σ_x and y_j/σ_x are independent unit-variance normal random variables. By well-known properties of the χ^2 distribution, $\mathrm{var}(r_j^2) = \langle r_j^2 \rangle^2$ and thus $\mathrm{var}[S(\nu_j)] = \langle S(\nu_j) \rangle^2$.

ALTERNATIVE DERIVATION OF EQ. (3)

Here we give a proof of Eq. (3) using the error propagation formula, which may provide insights not evident in the more abstract treatment using Fisher information. As in the main text, the spectrum is described by a multivariate normal distribution with mean $\langle \bar{S}_i \rangle = f(\nu_i, \mathbf{v}) \equiv f_i$, variance $\mathrm{var}(\bar{S}_i) = f_i/\mathcal{N}$ and cross-correlations $\mathrm{cov}(\bar{S}_i, \bar{S}_j) = 0$ for $i \neq j$. Maximum likelihood estimation is performed by minimizing $\chi^2 \equiv \sum_i (f_i - \bar{S}_i)^2/(\mathcal{N} f_i)$, i.e., finding $\hat{\mathbf{v}}$ such that

$$\partial_j \chi^2(\mathbf{v})\big|_{\mathbf{v}=\hat{\mathbf{v}}} = 0 \tag{8}$$

where ∂_j indicates $\partial/\partial v_j$ and v_j is a component of the parameter vector $\mathbf{v}$. Applying the derivative, the optimization condition can be written (we use the Einstein summation convention from here forward)

$$\left.\frac{(f_i - \bar{S}_i)\partial_j f_i}{f_i^2}\right|_{\mathbf{v}=\hat{\mathbf{v}}} = \left.\frac{(f_i - \bar{S}_i)^2 \partial_j f_i}{f_i^3}\right|_{\mathbf{v}=\hat{\mathbf{v}}}. \tag{9}$$

We can apply the variational principle to understand how a small error in $\bar{S}_i$ i.e. $\bar{S}_i = f_i + \delta\bar{S}_i$ produces a corresponding error in the estimator $\hat{v}_k = v_k + \delta v_k$. The r.h.s. of Eq. (9) is of order $(\delta\bar{S}_i)^2$ and thus vanishingly small compared to the l.h.s. in the asymptotic limit. The l.h.s. similarly vanishes, maintaining the optimum, provided that

$$\frac{(\partial_k f_i)(\partial_j f_i)}{f_i^2}\delta\hat{v}_k = \frac{\partial_j f_i}{f_i^2}\delta\bar{S}_i \tag{10}$$

At this point it is convenient to introduce the matrices

$$L_{ij} \equiv \frac{\partial_j f_i}{f_i} \tag{11}$$

and

$$M_{jk} \equiv L_{ji}L_{ki} = \frac{(\partial_k f_i)(\partial_j f_i)}{f_i^2} \tag{12}$$

We note the relation to the Fisher information of Eq. (3): $\mathcal{I} = (\mathcal{N}+2)M$. Equation (10) then becomes

$$M_{jk}\delta\hat{v}_k = L_{ji}\frac{\delta\bar{S}_i}{f_i} \tag{13}$$

with solution

$$\delta\hat{v}_k = M_{kj}^{-1}L_{ji}\frac{\delta\bar{S}_i}{f_i}. \tag{14}$$

The elements of the covariance matrix of $\hat{\mathbf{v}}$ are given by:

$$\begin{aligned}\Gamma_{jk} &\equiv \langle \hat{v_j}\hat{v}_k\rangle - \langle \hat{v_j}\rangle\langle \hat{v}_k\rangle = \langle \delta\hat{v_j}\delta\hat{v}_k\rangle \\ &= \left\langle \frac{M_{jl}^{-1}L_{lm}\delta\bar{S}_m (M_{kn}^{-1}L_{np}\delta\bar{S}_p)}{f_m f_p}\right\rangle \\ &= \left\langle M_{jl}^{-1}L_{lm}L_{pn}M_{nk}^{-1}\frac{\delta\bar{S}_m\delta\bar{S}_p}{f_m f_p}\right\rangle \end{aligned} \tag{15}$$

Using

$$\langle \delta\bar{S}_m \delta\bar{S}_p\rangle = f_m f_p \delta_{mp}/\mathcal{N} \tag{16}$$

we obtain:

$$\begin{aligned}\Gamma_{jk} &= M_{jl}^{-1}L_{lm}L_{pn}M_{nk}^{-1}\delta_{mp}\mathcal{N}^{-1} \\ &= M_{jk}^{-1}\mathcal{N}^{-1}\end{aligned} \tag{17}$$

which approaches Eq. (3) of the main text for large $\mathcal{N}$.

SPECTRAL PARAMETERS VERSUS OPTICAL POWER AND ATOMIC DENSITY

As described in detail in [35], the parameters $(S_{\mathrm{ph}}, \nu_L, S_{\mathrm{at}}, \Delta\nu)$ can be computed from first principles. The contribution from photon shot-noise to the spin noise spectrum $S(\nu)$ is given by:

$$S_{\mathrm{ph}} = 2G^2 q(\Re P)\xi^2, \tag{18}$$

where ξ^2 is the squeezing factor, $G = 10^6$ V/A is the transimpedance gain, P is the total optical power reaching the detector, $\Re = \eta q/E_{\mathrm{ph}}$ is the detector responsivity, η denotes the quantum-efficiency of the detector, $E_{\mathrm{ph}} = \hbar\omega = 2.49\times10^{-19}$ J is the photon energy at

795 nm, and $q = 1.6 \times 10^{-19}$ C is the electron charge. The on-resonance contribution from the atomic ^{85}Rb spin noise is given by:

$$S_{\rm at} = \frac{8G^2(\Re P)^2\kappa^2 A_{\rm eff} L_{\rm cell} n^{(87)}}{\pi\Delta\nu} \tag{19}$$

where $A_{\rm eff} = 0.054$ cm^2 is the effective area, $L_{\rm cell} = 3$ cm is the vapor cell length and κ^2 is a parameter including the spectral factor, defined in Eq. (13) of [35]. $n^{(87)} = 0.72n$ is the number density of ^{85}Rb at natural abundance. The FHWM linewidth is given by

$$\Delta\nu = \frac{1}{T_2\pi} = \frac{1}{\pi}(\Gamma_0 + \alpha n + \beta P) \tag{20}$$

where Γ_0 is the unperturbed relaxation rate, α and β are collisional and power broadening factors, respectively. Finally, the Larmor frequency $\nu_L = \gamma B$, where γ is the gyromagnetic ratio and B is the magnetic field strength. In our range of parameters, ν_L is not significantly affected by light shifts or collisional shifts and is taken as constant. Numerical values of the defined variables, for our experimental conditions, could be found in Table I in [35].

SENSITIVITY TO SHOT NOISE LEVEL $\Gamma_{11}^{\rm th}(n,P)$ AND PEAK ATOMIC NOISE $\Gamma_{33}^{\rm th}(n,P)$

In Fig. (5) we show 2D contour-plots of the variances of the estimated atomic $S_{\rm at}$ and shot noise $S_{\rm ph}$ contributions to the power spectrum, given by the covariance matrix diagonal terms $\Gamma_{33}^{\rm th}(n,P)$ and $\Gamma_{11}^{\rm th}(n,P)$, respectively.

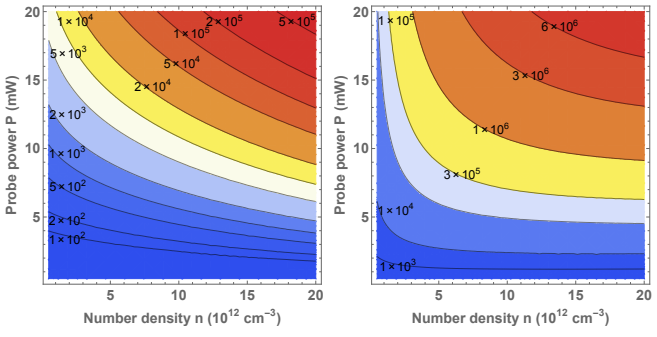

FIG. 5. $\Gamma_{11}^{\rm th}$ (left), variance in shot noise power spectral density and $\Gamma_{33}^{\rm th}$ (right), variance in peak spin noise power spectral density, as predicted by Eq. (3) as a function of number density and probe power. Both in units of μV^4/Hz^2.

For these fit parameters the theoretical variance increases monotonically with both power and density, without showing an optimal region or an inversion trend within the investigated parameter range, differently from the variance of the estimated Larmor frequency ν_L and resonance linewidth $\Delta\nu$, as shown in the main paper.

CALCULATION OF EXPERIMENTAL VARIANCES AND THEIR UNCERTAINTIES

The variances from experimental observations are computed as $\Gamma_{ii}^{\rm exp} = k_2$, the second "k-statistic," i.e., Fisher's unbiased estimator for the second cumulant. k_2 and k_4, fourth k-statistic, are computed from m observations $v^{(1)}, \ldots, v^{(m)}$ as

$$k_2 = \frac{m(S_2 - S_1^2)}{m(m-1)} \tag{21}$$

and

$$k_4 = \frac{-6S_1^4 + 12mS_1^2S_2 - 3m(m-1)S_2^2}{m(m-1)(m-2)(m-3)} + \frac{-4m(m+1)S_1S_3 + m^2(m+1)S_4}{m(m-1)(m-2)(m-3)} \tag{22}$$

where

$$S_r \equiv \sum_{i=1}^{m} (v^{(i)})^r. \tag{23}$$

The estimated variance in k_2 is then calculated using the unbiased estimator for var(k_2) [50, pp. 189-190] :

$$\mathrm{var}(\Gamma_{ii}^{\rm exp}) = \mathrm{var}(k_2) = \frac{2nk_2^2 + (n-1)k_4}{n(n+1)}. \tag{24}$$

From Eq. (24) we obtain the standard error of the diagonal elements of the sample covariance matrix $\Gamma_{ii}^{\rm exp}$.